JOURNAL OF MATERIALS SCIENCE **40** (2005) 6459–6462

Microstructure development and nonlinear electrical characteristics of the SnO_2·CuO·Ta_2O_5 based varistors

CHUN-MING WANG*, JIN-FENG WANG, WEN-BIN SU, HONG-CUN CHEN, GUO-ZHONG ZANG, PENG QI
School of Physics and Microelectronics, National Key Laboratory of Crystal Materials, Shandong University, Jinan 250100, People's Republic of China
E-mail: sdwangcm@mail.edu.cn, sdwangcm@mail.sdu.edu.cn

Published online: 5 October 2005

The microstructure development of SnO_2·CuO based ceramic material was analyzed by XRD and SEM and the electrical properties were investigated by *J-E* relation. The secondary phases of copper oxide were found by the XRD. Copper oxide could make tin oxide densify and advance the grain growth, while tantalum oxide would retard the grain growth. Excess copper would centralize at the grain boundaries and prevent the mass transport. The high nonlinear coefficient ($\alpha = 27.3$) and low leakage current density ($J_L =$ 16 μA cm^{-2}) for the 0.05 mol% Ta_2O_5-doped SnO_2·CuO based varistor sample were obtained. The modified defect barrier model for CuO and Ta_2O_5-doped SnO_2 based varistors was introduced.

In the past decade, tin oxide as varistors has been extensively studied experimentally and theoretically, since this oxide similar to zinc oxide varistors shows nonlinearity when doped with minor other oxides, such as CoO, ZnO, Ni_2O_3, Ta_2O_5, Nb_2O_5 and rare-earth oxides [1–8]. It is found, from the recent publications, that zinc oxide [2, 3] or nickel oxide [4, 5] doped SnO_2-based varistors showed the modest nonlinearity and cobalt oxide is essential for SnO_2-based varistors that possess excellent nonlinearity and higher density [1, 6–8]. Recently, we found that CuO-doped SnO_2 ceramic system also shows excellent nonlinearity and low leakage current.

In this letter, the microstructure and nonlinear electrical properties of the varistor system SnO_2·CuO·Ta_2O_5 (named SCT) are investigated, for the appearance of other phases and their excellent nonlinearity. The appearance of other phases is a very interesting phenomenon and contrary to the generally accepted single-phase microstructure of SnO_2 varistor material. Some satisfying results and the high nonlinear coefficient ($\alpha = 27.3$) are obtained. The relative density of the varistor samples is up to 94% of the theoretical density.

The materials used in the present study were analytical grades of SnO_2 (analytical grades, 99.5% purity), CuO (98.0%) and Ta_2O_5 (99.5%). Tin oxide varistors were prepared from samples containing selected metal oxides (see Table I) and produced by the conventional ceramic fabrication procedure reported earlier [7, 8]. They were sintered at 1400°C for 1 h and cooled to room temperature freely. The ceramic phases analysis was conducted by X-ray diffraction (XRD, XD-3, PGeneral) patterns. Density (ρ) measurements were carried out using the Archimedes method. Microstructure characterization of the sintered ceramics was conducted by scanning electron microscopy (SEM, JXA-840, JEOL). The grain sizes (d) were calculated by microstructure linear analysis. For the direct-current density-electrical field (*J-E*) characterization, silver electrodes (1 cm^2) were made on both surfaces of the sintered discs and fired for 20 min at 550°C in air. A 2410 High-Voltage SourceMeter (Keithley) was used for *J-E* measurement. The dielectric loss (tanδ) measurements were performed with an HP4294A (Agilent) impedance analyzer.

The SEM photomicrographs of the pure SnO_2 (S0), SnO_2·CuO (SCu) and SnO_2·CuO·Ta_2O_5 (SCT005 and SCT025) ceramic systems are presented in Fig. 1. In S0 (pure SnO_2) sample, many pores occur; while in other samples, the grains are tightly close together with minor other phases in grain boundaries. Therefore, the SEM

TABLE I Sample compositions

Samples	SnO_2 (mol%)	CuO (mol%)	Ta_2O_5 (mol%)
S0	100.00	–	–
SCu	99.00	1.00	–
SCT005	98.95	1.00	0.05
SCT025	98.75	1.00	0.25
SCT050	98.50	1.00	0.50

*Author to whom all correspondence should be addressed.
0022-2461
DOI: 10.1007/s10853-005-1709-1

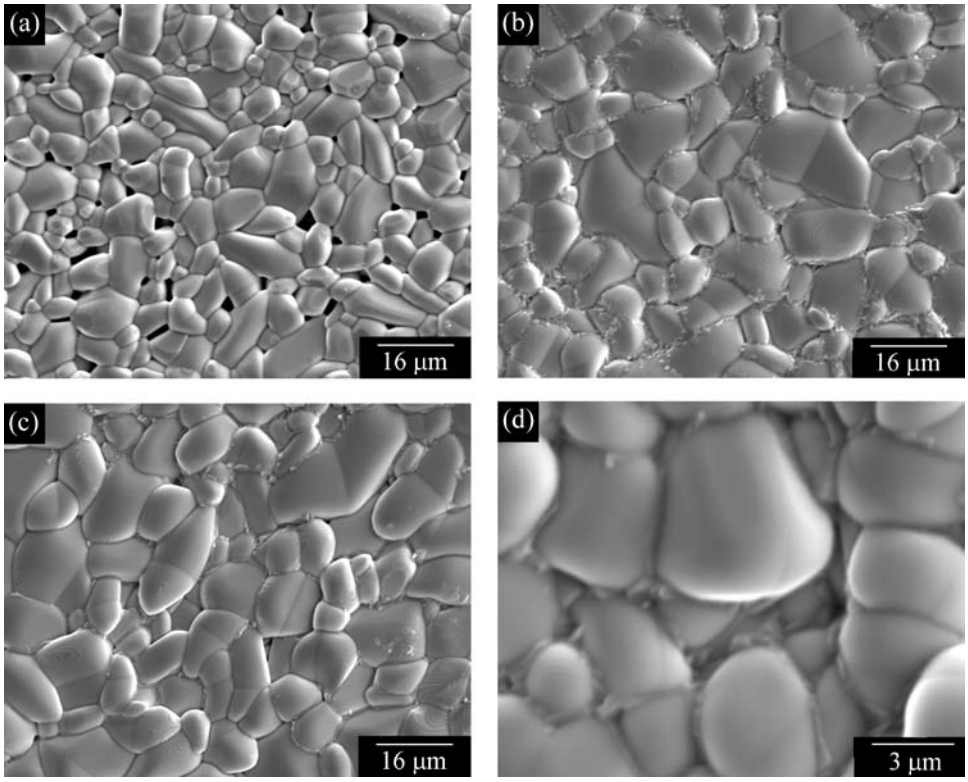

Figure 1 SEM images of the ceramic systems: (a) S0, (b) SCu, (c) SCT005, (d) SCT025.

photomicrographs also reveal the density of the samples doped with copper oxide is more denser than that of pure tin oxide. The phenomenon of the appearance of other phases in the grain boundaries is distinct from the single phase of SnO_2·CoO [7, 8] based ceramic systems previously reported, which is an interesting thing. This may be explained by the low melting point of copper oxide and the improvement of the sintering temperature. The copper oxide into tin oxide is up to saturation, and excess copper oxide that could not enter into tin oxide lattice would centralize at the grain boundaries and prevent the mass transport, which was also investigated and confirmed by Nisiro *et al*. [9]. However, SnO_2·CuO ceramic system is highly resistive, showing no signs of nonlinearity, though it is highly denser than pure SnO_2. Table II lists the density and the relative theoretical density (ρ_{rt}) for all the ceramic samples. The relative theoretical density (ρ_{rt}) is obtained by the Archimedes method and related to the theoretical density of the SnO_2 ($= 6.95 g\ cm^{-3}$). As discussed in pervious literatures [7, 8], due to the high vapor pressure of tin oxide, it does not densify during sintering. The density of tin oxide sintered at above-mentioned condition is 5.55 g cm^{-3}, 79.9% of the theoretical density. However, the high densification of tin oxide ceramic material could be obtained by doping with the 1.00 mol% CuO additives, which was attributed to the copper oxide effect in the tin oxide lattice. Table II presents the average grain size of all the ceramic systems. It can be seen the grain size is bigger than that of pure SnO_2, which shows the copper oxide advances the tin oxide grain growth. But with the increase of tantalum content, the grain size drastically decreases. This is similar to the CoO and Ta_2O_5-doped SnO_2 varistors wherein grain size significantly drops with increasing tantalum content [7].

The surface XRD patterns of selected samples are shown in Fig. 2. The JCPDS cards (SnO_2: 77-0451; CuO: 80-1916; Ta_2O_5: 73-2323) were used in the analysis of the phases within the samples. The XRD data reveal that only the rutile tin oxide lines were found in the S0 sample (pure SnO_2). In the copper oxide doped samples (SCu), additional peaks are evident, which reveals only a few copper oxide dissolve into tin oxide lattice, while mass congregate at the grain boundaries. However, no tantalum oxide peak is found in Ta_2O_5 and CuO-doped tin oxide (SCT050 as a representative). Furthermore, from the Fig. 2, it can be seen that the sample with the dopant of Ta_2O_5 exhibits much stronger secondary phase (CuO). This is maybe due to the addition of Ta^{5+}, which will take up the position of

TABLE II Microstructural and electrical characteristic parameters of tin oxide ceramic materials

Samples	ρ^a (g cm^{-3})	$\rho_{rt}{}^a$ (%)	d (μm)	α	E_B (kV m^{-1})	J_L (μA cm^{-2})	tanδ (1 kHz)
S0	5.55	79.9	11.5	–	–	–	–
SCu	6.72	96.7	17.4	–	–	–	0.028
SCT005	6.55	94.2	16.5	27.3	750	16	0.016
SCT025	6.56	94.3	6.8	4.6	286	352	0.121
SCT050	6.88	98.9	5.0	2.3	151	596	0.595

[a]The theoretical density of SnO_2 is 6.95 g cm^{-3}

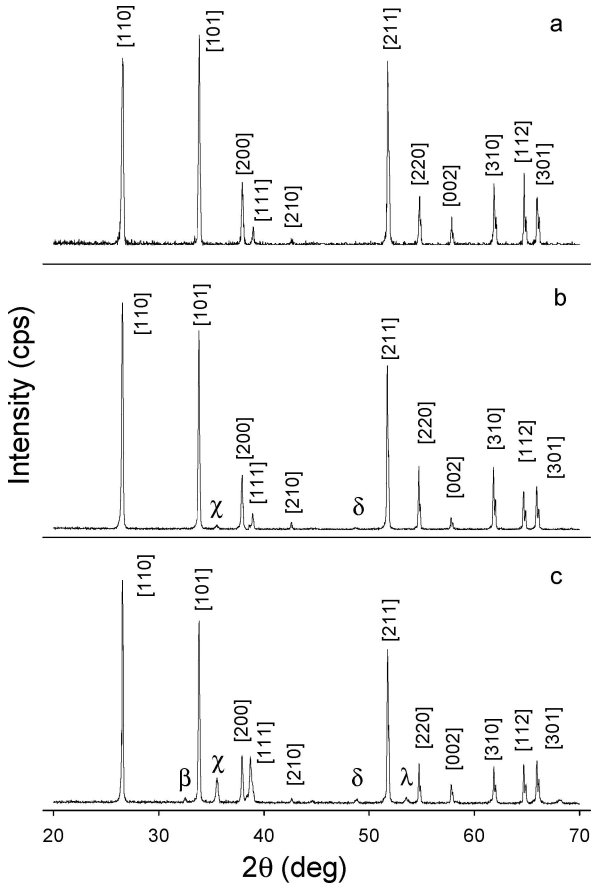

Figure 2 X-ray diffraction patterns of the ceramic samples: (a) S0, (b) SCu and (c) SCT050. Note: SnO_2 peaks and additional peaks β: CuO [110], χ: CuO [$\bar{1}$11], δ: CuO [$\bar{2}$02] and λ: CuO [220].

Cu^{2+} inside the tin oxide lattice and push the copper ions out of the grain. Thus, tantalum will enter into grains and make the grains conductive. This process may be described by the equation [7]:

$$Ta_2O_5 \xrightarrow{SnO_2} 2Ta_{Sn}^{\cdot} + 2e' + xO_O^{\times} + \frac{5-x}{2}O_2, \quad x = 0-5 \qquad (1)$$

where the Kröger-Vink marks were used. Therefore, the Ta_2O_5 addition to the SnO_2 lattice leads to an increase in the electronic conductivity in the grain, which also is seen from the decrease of breakdown electrical filed (E_B) listed in Table II. The breakdown electrical field E_B was measured at a current density of 10 A m^{-2} and the leakage current density (J_L) was measured at 0.75 E_{10A}. As the important parameter, the nonlinear coefficient (α) was obtained by the following equation:

$$\alpha = \frac{\log J_2 - \log J_1}{\log E_2 - \log E_1} \qquad (2)$$

where $J_1 = 10$ A m^{-2}, $J_2 = 100$ A m^{-2} and E_1 and E_2 are the electrical fields corresponding to J_1 and J_2, respectively. These varistor parameters are listed in Table II. The SCT005 varistor sample has the high nonlinear coefficient ($\alpha = 27.3$) and low leakage current density ($J_L = 16$ μA cm^{-2}), which is very beckoning and worth to further investigation.

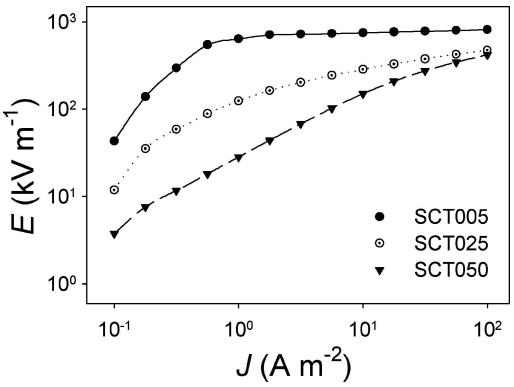

Figure 3 *J-E* characteristics of the varistor samples.

The plots of the current density against the applied electrical field for the varistor material samples are shown in Fig. 3. It is found that the SCT005 sample has the best linear electrical property and the slope of quasilinear curve is very low in the current density range from 1 to 100 A m^{-2}, which are consistent with that the sample has the highest nonlinear coefficient ($\alpha = 27.3$) in all samples. Whereas the slopes of other quasilinear curves are sizable and the nonlinear coefficient of other samples is ~10, therefore, effects to further improve the nonlinearity are in progress. Fig. 4 shows the dielectric loss (tanδ) versus frequency plots for the SCu and SCT samples. The dielectric loss decreases with frequency increase in the range 100 Hz–10 MHz. As can be seen, the dielectric loss for SCT005 sample is lower than 0.03, which is fine for the SnO_2-based varistors. The dielectric loss for SCT025 and SCT050 samples is extremely high in the frequency range of 100 Hz–10 kHz. The values of tanδ at 1 kHz for all samples are listed in Table II.

The generally accepted microstructure of SnO_2 varistor material is single phase by SEM and XRD, which is different from that of ZnO varistor material which has been extensively studied and considered a multiphase one being the ZnO grains as predominant and several secondary phases as the spinel phase ($Zn_7Sb_2O_{12}$), pyrochlore ($Zn_2Bi_3Sb_3O_{14}$) and a polymorphic phase of bismuth oxide. The reason for no other phases in tin oxide varistors is commonly due to the little additive added and the low resolving power of normal X-ray diffraction [1–3, 7]. And the nonlinearity of tin oxide varistors is attributes to the adsorbed oxygen species and minor possible other phases. By SEM and XRD, the CuO and

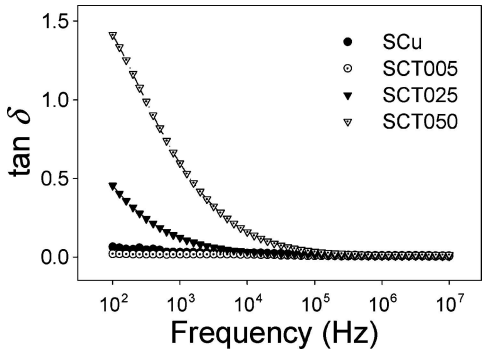

Figure 4 Dielectric loss versus frequency for the ceramic samples.

Ta_2O_5-doped tin oxide varistors are found to be SnO_2 grains as predominant and minor copper oxide at grain boundaries, while tantalum improves the conductive of the grains. The copper oxide intergranular insulating layer separates two semi-conductive tin oxide grains and forms the barriers. The electric transport occurs by tunneling across the barriers and is responsible for the electrical nonlinearity of the varistors. Further, the oxygen will be partly adsorbed at SnO_2 grain boundaries and adsorbed oxygen may easily capture electrons or react with partial negatively charged defects to become negatively charged ions:

$$O_2 \rightarrow 2O_{ad}^{x} \tag{3}$$

$$O_{ad}^{x} + e' \rightarrow O'_{ad} \tag{4}$$

These negatively charged adsorbed oxygen species are essential to the Schottky barrier formation and also responsible for the electrical nonlinearity of the varistors. The role of the adsorbed oxygen in the formation of boundary barriers was confirmed by literatures [10, 11].

In conclusion, copper oxide could greatly make tin oxide densify. Furthermore, the introduction of minor donors tantalum into SnO_2·CuO ceramic system would make it possess excellent nonlinearity. The microstructure development of SnO_2·CuO based ceramic material was analyzed by XRD and SEM and the electrical properties were investigated by *J-E* relation. Copper oxide could advance the tin oxide grain growth, while tantalum oxide would retard the grain growth. Excess copper would centralize at the grain boundaries and prevent the mass transport. The excellent nonlinearity ($\alpha = 27.3$) and low leakage current density ($J_L = 16\,\mu A\,cm^{-2}$) for the SCT005 sample was obtained. The varistor system of SnO_2·CuO·Ta_2O_5 would be worth of further investigation.

Acknowledgment

Supported by the Natural Science Foundation of Shandong Province of China under the Grant No Z2003F04.

References

1. S. A. PIANARO, P. R. BUENO, E. LONGO and J. A. VARELA, *J. Mater. Sci. Lett.* **14** (1995) 692.
2. Y. J. WANG, J. F. WANG, C. P. LI, H. C. CHEN, W. B. SU, W. L. ZHONG, P. L. ZHANG and L. Y. ZHAO, *ibid.* **20** (2001) 19.
3. J. F. WANG, Y. J. WANG, W. B. SU, H. C. CHEN and W. X. WANG, *Mat. Sci. Eng.* B **96** (2002) 8.
4. C. P. LI, J. F. WANG, W. B. SU, H. C. CHEN, W. X. WANG, D. X. ZHUANG and L. XU, *Eur. Phys. J. Appl. Phys.* **16** (2001) 3.
5. J. F. WANG, H. C. CHEN, W. X. WANG, W. B. SU and G. Z. ZANG, *Mat. Sci. Eng.* B **99** (2003) 465.
6. A. C. ANTUNES, S. R. M. ANTUNES, S. A. PIANARO, M. R. ROCHA, E. LONGO and J. A. VARELA, *J. Mater. Sci. Lett.* **17** (1998) 577.
7. C. M. WANG, J. F. WANG, H. C. CHEN, W. X. WANG, W. B. SU, G. Z. ZANG and P. QI, *J. Phys.* D*: Appl. Phys.* **36** (2003) 3069.
8. C. M. WANG, J. F. WANG, H. C. CHEN, W. B. SU, G. Z. ZANG, P. QI and B. Q. MING, *Solid State Commun.* **132** (2004) 163.
9. D. NISIRO, G. FABBRI, G. C. CELOTTI and A. BELLOSI, *J. Mater. Sci.* **38** (2003) 2727.
10. F. STUCKI and F. GREUTER, *Appl. Phys. Lett.* **57** (1990) 446.
11. P. R. BUENO, E. R. BEITE, M. M. OLIVEIRA, M. O. ORLANDI and E. LONGO, *ibid.* **79** (2001) 48.

Received 6 January
and accepted 26 April 2005